On the ill-conditioning of the combined wind speed estimator and tip-speed ratio tracking control scheme

Brandetti, L.; Liu, Y.; Mulders, S. P.; Ferreira, C.; Watson, S.; Van Wingerden, J. W.

DOI
10.1088/1742-6596/2265/3/032085

Publication date
2022

Document Version
Final published version

Published in
Journal of Physics: Conference Series

On the ill-conditioning of the combined wind speed estimator and tip-speed ratio tracking control scheme

On the ill-conditioning of the combined wind speed estimator and tip-speed ratio tracking control scheme

L Brandetti[1,2], Y Liu[2], SP Mulders[2], C Ferreira[1], S Watson[1], JW van Wingerden[2]

[1]AWEP Department, Faculty of Aerospace Engineering, Delft University of Technology, Delft, The Netherlands.
[2]DCSC Department, Faculty of Mechanical, Maritime and Materials Engineering, Delft University of Technology, Delft, The Netherlands.

E-mail: l.brandetti@tudelft.nl

Abstract. In recent years, industrial controllers for modern wind turbines have been designed as a combined wind speed estimator and tip-speed ratio (WSE-TSR) tracking control scheme. In contrast to the conventional and widely used $K\omega^2$ torque control strategy, the WSE-TSR scheme provides flexibility in terms of controller responsiveness and potentially improves power extraction performance. However, both control schemes heavily rely on prior information about the aerodynamic properties of the turbine rotor. Using a control-oriented linear analysis framework, this paper shows that the WSE-TSR scheme is inherently ill-conditioned. The ill-conditioning is defined as the inability of the scheme to uniquely determine the wind speed from the product with other model parameters in the power balance equation. Uncertainty of the power coefficient contribution in the latter mentioned product inevitably leads to a biased effective wind speed estimate. As a consequence, in the presence of uncertainty, the real-world wind turbine deviates from the intended optimal operating point, while the controller believes that the turbine operates at the desired set-point. Simulation results confirm that inaccurate model parameters lead to biased estimates of the actual turbine operating point, causing sub-optimal power extraction efficiency.

1. Introduction

Wind energy plays a crucial role in the global energy mix as its installed power capacity continues to increase [1]. After the Glasgow climate summit, the net-zero emissions targets set for the middle of the century pose ambitious goals for the wind industry [2]. To efficiently achieve these goals, the sizes of wind turbines increase dramatically. Larger turbines together with a more flexible rotor assembly and support structure result in a rising demand for optimization of wind turbine controllers [3].

Modern wind turbines usually employ a variable-speed variable-pitch (VS-VP) operating strategy, and thereby use generator torque control to maximize energy capture in below-rated operating conditions [4, 5]. Until recently, the most common partial load wind turbine torque control strategy is the so-called $K\omega^2$ controller, being a fixed mapping as a function of the generator speed [6]. This control scheme has a predefined control responsiveness and relies heavily on modeled aerodynamic rotor characteristics. As a partial solution, current practice in industrial controllers for modern turbines is to use a combined wind-speed estimator and tip-speed ratio (WSE-TSR) tracking control scheme.

The TSR tracker aims to maximize and improve on power extraction by employing a dynamical controller implementation, allowing for an adaptable control responsiveness compared to the conventional $K\omega^2$ controller [7, 4]. The WSE-TSR tracking control scheme typically

includes a wind speed estimator, that, like the $K\omega^2$ controller, relies on information about aerodynamic rotor characteristics and other (environmental) properties. Inaccuracy in this information inevitably leads to biased wind speed estimates, resulting in sub-optimal turbine operation by the TSR tracking controller.

This paper shows that the WSE-TSR tracking control scheme is still highly dependent on prior information about the wind turbine. More specific, the TSR tracker lacks information when coupled with a wind speed estimator giving rise to the so-called ill-conditioning described in this paper. This ill-conditioning prevents a unique estimation of the wind speed from the product with other model parameters in the power balance equation, and hinders the determination of the true turbine operating point. For the case under study, uncertainty in the power coefficient mapping results in a biased wind speed estimate from the actual effective wind speed. Because the estimated wind speed is subsequently used in the calculation of the feedback signal to the TSR tracker, this difference results in sub-optimal operational performance of the real-world turbine. In contrast, the controller believes to satisfy the desired optimal operating condition.

To the authors' knowledge, no detailed study of the WSE-TSR tracking control scheme is available in the literature. To this end, the current research outlines how the framework is generally implemented and thereby presents the following contributions:

- Formalizing the problem of ill-conditioning, showing that this leads to steady-state biased wind speed (and thus tip-speed ratio) estimates and thus sub-optimal power tracking.
- Providing an analytical frequency-domain framework which gives an in-depth analysis of the working mechanisms of the controller, and which is used to analyze the problem of ill-conditioning.

The paper is structured as follows: Section 2 gives a mathematical overview of the WSE-TSR tracking control scheme together with the assumptions made when analysing the scheme. The problem of ill-conditioning is formalized in Section 3. Section 4 presents the frequency-domain framework used to analyze the WSE-TSR scheme and the problem of ill-conditioning by deriving the most relevant transfer functions. Both a time-domain and a frequency-domain analysis of the framework is performed in Section 5 for different uncertainty in the modeled parameters. Finally, Section 6 summarizes the main findings and recommendations for future work.

2. Methodology

While the exact implementation might differ between turbines, the general framework of the WSE-TSR control scheme is outlined in this section and is used for analysis throughout the paper. As illustrated in Figure 1, the framework consists of the wind turbine, the rotor-effective wind speed estimator and the controller. The red box highlights the real wind turbine system with two inputs (the generator torque T_g, and the wind speed V), and with two outputs (the rotational speed ω_r, and the TSR λ). The measured T_g and ω_r are used to estimate the rotor-effective wind speed $\hat{V}$ and to calculate an estimate of the TSR $\hat{\lambda}$, in the estimator block. The estimated TSR is then fed back to the controller block to close the loop. By applying the TSR tracking control scheme, the turbine is ideally forced to operate at the optimal TSR λ^*, which corresponds to the rotor operating point for maximum power extraction efficiency C_p^*. In the following subsections, the wind turbine, the wind speed estimator and the controller are presented in detail together with the assumptions made when analysing the framework.

2.1. Assumptions

The first step in analysing the framework is the formulation of the assumptions, under which the WSE-TSR tracking control scheme is operated.

Assumption 1. *The WSE-TSR tracking scheme is analysed in the below-rated region with a constant (fine-)pitch angle β, where the power coefficient $C_{\mathrm{p}}(\cdot)$ is solely a function of the tip-speed ratio $\lambda := \omega_{\mathrm{r}} R/V$, with R being the rotor radius, ω_{r} the measured rotor speed, and V the rotor-effective wind speed.*

Assumption 2. *The generator torque T_{g}, and the rotational speed ω_{r}, are measured signals and the wind speed V, is an unknown positive signal.*

Assumption 3. *The equivalent inertia of the low-speed generator shaft J, the air density ρ, and the rotor swept area A_{rot}, are equal for the real wind turbine and for the estimator.*

Assumption 4. *The drive-train efficiency η, which is defined as the ratio between the generator power and the rotor power, is set to 1.*

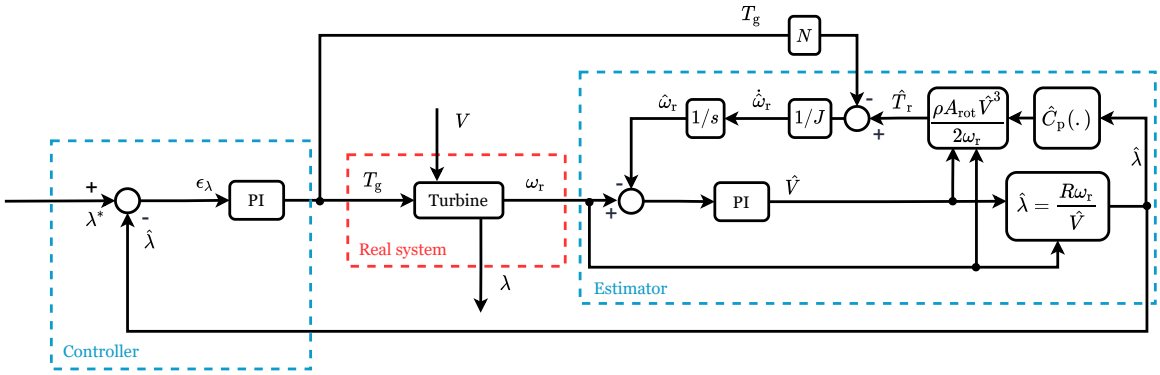

Figure 1: Block diagram of the WSE-TSR control framework: the wind turbine (*i.e.* the real system), the tip-speed ratio (TSR) tracker (*i.e.* the controller) and the wind speed estimator. The wind speed estimate $\hat{V}$, is used to calculate an estimation of tip-speed ratio $\hat{\lambda}$, which in turn is employed as a feedback signal to close the loop by the TSR tracking controller.

2.2. Wind turbine

The dynamics of the wind turbine are given by

$$J\dot{\omega}_{\mathrm{r}} = T_{\mathrm{r}} - T_{\mathrm{g}} N \,, \tag{1}$$

where J is obtained from the relation $J = J_{\mathrm{g}} N^2 + J_{\mathrm{r}}$. The inertias of the generator and rotor are J_{g} and J_{r}, respectively, and $N := \omega_{\mathrm{g}}/\omega_{\mathrm{r}}$ represents the gearbox ratio of the transmission with ω_{g} being the generator speed. According to Assumption 1, the aerodynamic rotor torque is given by

$$T_{\mathrm{r}} := \frac{1}{2} \rho A_{\mathrm{rot}} \frac{V^3}{\omega_{\mathrm{r}}} C_{\mathrm{p}}(\lambda) \,. \tag{2}$$

2.3. Estimator

The rotor-effective wind speed is estimated based on the extended Immersion and Invariance (I&I) estimator with a Proportional and Integral (PI) correction term [8, 9], which is illustrated in Figure 2. Note that $\hat{V}$ indicates the estimated wind speed, while $\bar{V}$ corresponds to the steady-state wind speed. Given Assumption 2, the wind speed estimator can be formulated as follows

$$\begin{cases} J\dot{\hat{\omega}}_{\mathrm{r}} = \hat{T}_{\mathrm{r}} - T_{\mathrm{g}} N \\ \epsilon_{\omega_{\mathrm{r}}} = \omega_{\mathrm{r}} - \hat{\omega}_{\mathrm{r}} \\ \hat{V} = K_{\mathrm{p,w}} \epsilon_{\omega_{\mathrm{r}}} + K_{\mathrm{i,w}} \int_0^t \epsilon_{\omega_{\mathrm{r}}}(\tau) \mathrm{d}\tau \end{cases} , \tag{3}$$

with t being the present time, τ the variable of integration, $K_{\mathrm{p,w}}$ the proportional gain and $K_{\mathrm{i,w}}$ the integral gain of the estimator. By adding the integrator, the extended formula given by

Equation (3) forces the error ϵ_{ω_r} to converge to zero, providing consistent estimates of not only the wind speed, but also of the rotor speed $\hat{\omega}_r$ [8]. The estimated aerodynamic torque is defined as

$$\hat{T}_r := \frac{1}{2}\rho A_{rot}\frac{\hat{V}^3}{\omega_r}\hat{C}_p(\hat{\lambda})\,. \tag{4}$$

In this case, $\hat{C}_p$ is the estimated power coefficient and the nonlinear mapping $\hat{C}_p(\cdot)$ is a function of the estimated TSR $\hat{\lambda} := \omega_r R/\hat{V}$.

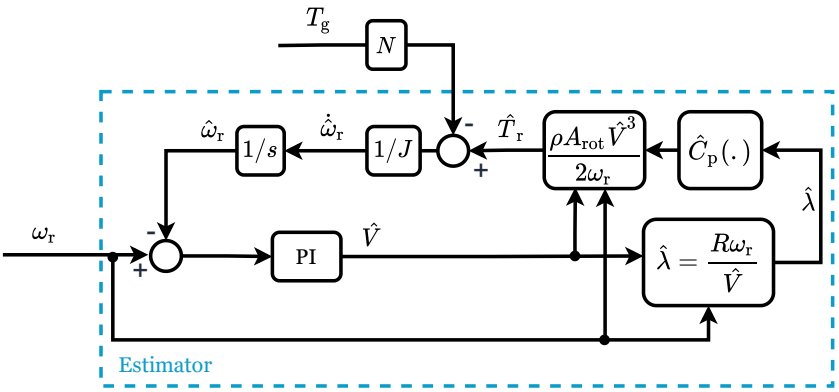

Figure 2: Block diagram of the extended I&I estimator with a Proportional and Integral (PI) correction term [8, 9]. The measured generator torque T_g, and rotational speed ω_r, are used to estimate the rotor-effective wind speed $\hat{V}$, and to calculate an estimate of TSR $\hat{\lambda}$.

2.4. Control strategy

A simple PI controller, acting on the TSR error, $\epsilon_\lambda := \lambda^* - \hat{\lambda}$, is used to calculate a generator torque demand to track λ^* as

$$T_g = K_{p,c}\epsilon_\lambda + K_{i,c}\int_0^t \epsilon_\lambda(\tau)\mathrm{d}\tau\,, \tag{5}$$

where $K_{p,c}$ and $K_{i,c}$ are the proportional and integral gains of the TSR tracking controller, respectively [4].

3. Formulation of the ill-conditioning

Upon closer inspection, the framework is found to be ill-conditioned. This section reveals the cause of the ill-conditioning, and thus formulates the problem.

Ideally, in steady-state conditions and under Assumption 4, when the TSR tracker is applied, the actual aerodynamic rotor power P_r, equals the desired power P_d, that results as a set-point from the control scheme. This observation is mathematically formalized by:

$$P_r = P_d \qquad \rightarrow \qquad \frac{1}{2}\rho A_{rot}V^3 C_p(\lambda) = \frac{1}{2}\rho A_{rot}\hat{V}^3\hat{C}_p(\hat{\lambda})\,. \tag{6}$$

With Assumption 3, Equation (6) is simplified as:

$$V^3 C_p(\lambda) = \hat{V}^3\hat{C}_p(\hat{\lambda})\,. \tag{7}$$

Subject to a WSE-TSR tracking control scheme and in steady-state, Equation (7) should always be satisfied. Whilst the wind-speed-power-coefficient product is uniquely estimated, the individual values of the power coefficient and the wind speed cannot be uniquely estimated due to a lack of information in the framework, giving rise to the so-called ill-conditioning.

To further illustrate the effect of the ill-conditioning in the definition of the estimated quantities, the uncertainty in the model parameters is represented by:

$$\hat{V} := \frac{V}{\gamma^{1/3}}\,, \qquad \text{and} \qquad \hat{C}_\mathrm{p}(\hat{\lambda}) := \gamma C_\mathrm{p}(\lambda)\,, \tag{8}$$

with γ being a constant uncertainty factor. When $\hat{C}_\mathrm{p}(\hat{\lambda})$ differs from $C_\mathrm{p}(\lambda)$ then $\hat{V}$ will be biased to satisfy Equation (7). This is what defines the ill-conditioning problem when a WSE-TSR tracking control scheme is implemented. As will be shown in Sections 4 and 5, such ill-conditioning may introduce significant effects on the WSE-TSR tracking control scheme.

4. Frequency-domain framework

This section provides the analytical frequency-domain framework used to describe the working mechanisms of the WSE-TSR tracking control scheme, and to evaluate the problem of the ill-conditioning. To analyze the control scheme in the frequency domain, the dynamics of the nonlinear system are linearized at a specific operating point, defined by $(\bar{\omega}_\mathrm{r}, \bar{V})$. The relevant transfer functions are then derived and provided for the individual and combined subsystems in the subsequent sections. The resulting frequency-domain framework takes into account model uncertainty (Equation (8)) to study the problem of the ill-conditioning.

4.1. Wind turbine rotor dynamics

By applying Equation (1) at the linearization point and in terms of the Laplace variable s, an expression for the dynamic response of the turbine rotor can be obtained

$$\omega_\mathrm{r}(s)s = D\,\omega_\mathrm{r}(s) + E\,T_\mathrm{g}(s) + B\,V(s)\,, \tag{9}$$

where

$$D = \frac{1}{J}\frac{\partial T_\mathrm{r}}{\partial \omega_\mathrm{r}}\bigg|_{(\bar{\omega}_\mathrm{r},\bar{V})} = \frac{1}{2J}\rho A_\mathrm{rot}\left(-\frac{\bar{V}^3}{\bar{\omega}_\mathrm{r}^2}C_\mathrm{p}(\bar{\omega}_\mathrm{r},\bar{V}) + \frac{\bar{V}^2 R}{\bar{\omega}_\mathrm{r}}\,\frac{\partial C_\mathrm{p}(\omega_\mathrm{r},V)}{\partial\lambda}\bigg|_{(\bar{\omega}_\mathrm{r},\bar{V})}\right), \tag{10}$$

$$E = -\frac{1}{J}N\,, \tag{11}$$

$$B = \frac{1}{J}\frac{\partial T_\mathrm{r}}{\partial V}\bigg|_{(\bar{\omega}_\mathrm{r},\bar{V})} = \frac{1}{2J}\rho A_\mathrm{rot}\left(\frac{3\bar{V}^2}{\bar{\omega}_\mathrm{r}}C_\mathrm{p}(\bar{\omega}_\mathrm{r},\bar{V}) - \bar{V}R\,\frac{\partial C_\mathrm{p}(\omega_\mathrm{r},V)}{\partial\lambda}\bigg|_{(\bar{\omega}_\mathrm{r},\bar{V})}\right). \tag{12}$$

4.2. Estimator dynamics

Similarly, the estimated rotor speed dynamics are formulated as

$$\hat{\omega}_\mathrm{r}(s)s = \hat{D}\,\omega_\mathrm{r}(s) + E\,T_\mathrm{g}(s) + \hat{B}\,\hat{V}(s)\,, \tag{13}$$

where

$$\hat{D} = \frac{1}{J}\frac{\partial \hat{T}_\mathrm{r}}{\partial \omega_\mathrm{r}}\bigg|_{(\bar{\omega}_\mathrm{r},\bar{V})} = \frac{1}{2J}\rho A_\mathrm{rot}\left(-\frac{\bar{V}^3}{\bar{\omega}_\mathrm{r}^2}\hat{C}_\mathrm{p}(\bar{\omega}_\mathrm{r},\bar{V}) + \frac{\bar{V}^2 R}{\bar{\omega}_\mathrm{r}}\,\frac{\partial \hat{C}_\mathrm{p}(\omega_\mathrm{r},V)}{\partial\lambda}\bigg|_{(\bar{\omega}_\mathrm{r},\bar{V})}\right), \tag{14}$$

$$E = -\frac{1}{J}N\,, \tag{15}$$

$$\hat{B} = \frac{1}{J}\frac{\partial \hat{T}_\mathrm{r}}{\partial \hat{V}}\bigg|_{(\bar{\omega}_\mathrm{r},\bar{V})} = \frac{1}{2J}\rho A_\mathrm{rot}\left(\frac{3\bar{V}^2}{\bar{\omega}_\mathrm{r}}\hat{C}_\mathrm{p}(\bar{\omega}_\mathrm{r},\bar{V}) - \bar{V}R\,\frac{\partial \hat{C}_\mathrm{p}(\omega_\mathrm{r},V)}{\partial\lambda}\bigg|_{(\bar{\omega}_\mathrm{r},\bar{V})}\right). \tag{16}$$

Given Equation (3), the expression for $\hat{V}$ can also be written in the frequency domain as

$$\hat{V}(s) = \left(K_\mathrm{p,w} + \frac{K_\mathrm{i,w}}{s}\right)\left(\omega_\mathrm{r}(s) - \hat{\omega}_\mathrm{r}(s)\right). \tag{17}$$

4.3. Coupled wind turbine and estimator dynamics

The next step in the analysis is to derive the transfer function of the coupled wind turbine and estimator dynamics, as sketched in Figure 3. By combining Equations (9), (13) and (17), it is possible to express the estimated TSR as a function of T_g and V

$$\hat{\lambda}(s) = \frac{R}{\bar{V}}\omega_\mathrm{r}(s) - \frac{R\bar{\omega}_\mathrm{r}}{\bar{V}^2}\hat{V}(s) \tag{18}$$

$$= L_1(s)T_\mathrm{g}(s) + L_2(s)V(s) \tag{19}$$

$$= \hat{\lambda}_{T_\mathrm{g}}(s) + \hat{\lambda}_V(s)\,. \tag{20}$$

where $L_1(s)$ is the transfer function of $\hat{\lambda}$ to T_g

$$L_1(s) = \frac{\hat{\lambda}_{T_\mathrm{g}}(s)}{T_\mathrm{g}(s)} \tag{21}$$

$$= \frac{R\,E\left[s^2 + \left(\hat{B} - \frac{\bar{\omega}_\mathrm{r}}{\bar{V}}(D-\hat{D})\right)K_\mathrm{p,w}s + \left(\hat{B} - \frac{\bar{\omega}_\mathrm{r}}{\bar{V}}(D-\hat{D})\right)K_\mathrm{i,w}\right]}{\bar{V}(s-D)(s^2 + \hat{B}K_\mathrm{p,w}s + \hat{B}K_\mathrm{i,w})}\,, \tag{22}$$

and $L_2(s)$ is the transfer function of $\hat{\lambda}$ to V

$$L_2(s) = \frac{\hat{\lambda}_V(s)}{V(s)} \tag{23}$$

$$= \frac{R\,B\left(F_1 s^2 + F_2\,s + F_3\right)}{\bar{V}(s-D)(s^2 + \hat{B}K_\mathrm{p,w}s + \hat{B}K_\mathrm{i,w})}\,. \tag{24}$$

The terms $F_1 = \left(1 - \left(\bar{\omega}_\mathrm{r}/\bar{V}\right)K_\mathrm{p,w}\right)$, $F_2 = \left(\hat{B}K_\mathrm{p,w} + \left(\bar{\omega}_\mathrm{r}/\bar{V}\right)\hat{D}K_\mathrm{p,w} - \left(\bar{\omega}_\mathrm{r}/\bar{V}\right)K_\mathrm{i,w}\right)$ and $F_3 = \left(\hat{B} - \left(\bar{\omega}_\mathrm{r}/\bar{V}\right)\hat{D}\right)K_\mathrm{i,w}$ are used to make Equation (24) more compact.

By considering the effect of model uncertainty (Equation (8)), the wind speed estimator dynamics can be expressed as a function of the wind turbine dynamics as $\hat{D} = \gamma D$. According to the definition of ill-conditioning in Equation (7), the absence of model mismatch results in $\gamma = 1$, and $\hat{D} = D$. Thus, the transfer function $L_1(s)$ can be simplified as

$$L_1(s)\Big|_{\gamma=1} = \frac{R\,E}{\bar{V}(s-D)}\,. \tag{25}$$

On the other hand, if $\gamma \neq 1$, then $D - \hat{D} = D(1-\gamma)$. It follows that

$$L_1(s)\Big|_{\gamma\neq1} = \frac{R\,E\left[s^2 + \left(\hat{B} - \frac{\bar{\omega}_\mathrm{r}}{\bar{V}}D(1-\gamma)\right)K_\mathrm{p,w}s + \left(\hat{B} - \frac{\bar{\omega}_\mathrm{r}}{\bar{V}}D(1-\gamma)\right)K_\mathrm{i,w}\right]}{\bar{V}(s-D)(s^2 + \hat{B}K_\mathrm{p,w}s + \hat{B}K_\mathrm{i,w})}\,. \tag{26}$$

The following analysis employs the γ parameter to evaluate the effect of model uncertainty.

4.4. Coupled wind turbine and combined estimator-controller scheme dynamics

The closed-loop dynamics of the overall framework, illustrated in Figure 1, is obtained by coupling the wind turbine with the combined estimator-controller dynamics.

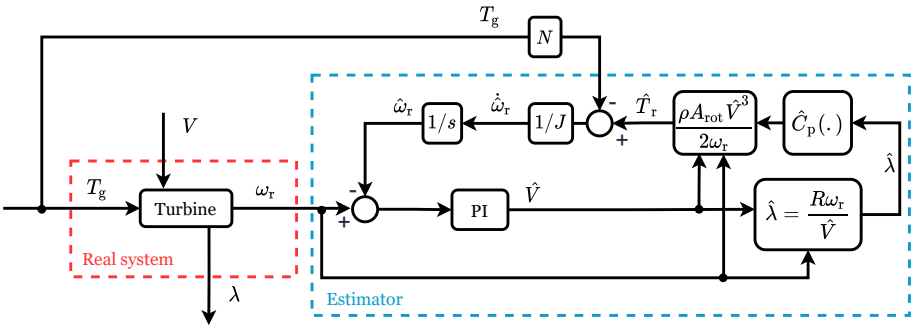

Figure 3: Block diagram of the coupled real system and the wind speed estimator. The measured generator torque T_g, and rotational speed ω_r, from the wind turbine are used to compute an estimate of the wind speed $\hat{V}$, and of the TSR $\hat{\lambda}$, in the estimator block.

By applying both the definition of ϵ_λ and Equation (5), the estimated TSR can be expressed as a function of λ^* and V to obtain the closed-loop dynamics of the system

$$\hat{\lambda}(s) = L_3(s)\lambda^*(s) + L_4(s)V(s) \tag{27}$$
$$= \hat{\lambda}_{\lambda^*}(s) + \hat{\lambda}_V(s)\,, \tag{28}$$

where $L_3(s)$ is the transfer function from $\hat{\lambda}$ to λ^*

$$L_3(s) = \frac{\hat{\lambda}_{\lambda^*}(s)}{\lambda^*(s)} = \frac{F_4}{\bar{V}s(s-D)(s^2 + \hat{B}K_{\mathrm{p,w}}s + \hat{B}K_{\mathrm{i,w}}) + F_4}\,, \tag{29}$$

and $L_4(s)$ is the transfer function from $\hat{\lambda}$ to V

$$L_4(s) = \frac{\hat{\lambda}_V(s)}{V(s)} = \frac{R\,B\left(F_1 s^2 + F_2 s + F_3\right)s}{\bar{V}s(s-D)(s^2 + \hat{B}K_{\mathrm{p,w}}s + \hat{B}K_{\mathrm{i,w}}) + F_4}\,, \tag{30}$$

with $F_4 = R\,E\left[s^2 + \left(\hat{B} - \left(\bar{\omega}_r/\bar{V}\right)D(1-\gamma)\right)K_{\mathrm{p,w}}s + \left(\hat{B} - \left(\bar{\omega}_r/\bar{V}\right)D(1-\gamma)\right)K_{\mathrm{i,w}}\right](K_{\mathrm{p,c}}s + K_{\mathrm{i,c}})$.

In the absence of model uncertainty, $\gamma = 1$, $L_3(s)$ can be simplified as

$$L_3(s)\Big|_{\gamma=1} = \frac{R\,E(K_{\mathrm{p,c}}s + K_{\mathrm{i,c}})}{\bar{V}s^2 + (R\,EK_{p,c} - \bar{V}D)s + R\,EK_{\mathrm{i,c}}}. \tag{31}$$

To analyze the ill-conditioning problem, it is also important to express the actual tip-speed ratio of the wind turbine λ, as a function of λ^* and V. By following the same derivation of Equations (18) and (27), this results in

$$\lambda(s) = L_5(s)\lambda^*(s) + L_6(s)V(s) \tag{32}$$
$$= \lambda_{\lambda^*}(s) + \lambda_{\mathrm{V}}(s), \tag{33}$$

where $L_5(s)$ is the transfer function from λ to λ^*

$$L_5(s) = \frac{\lambda_{\lambda^*}(s)}{\lambda^*(s)} = \frac{R\,E\left(s^2 + \hat{B}K_{\mathrm{p,w}}s + \hat{B}K_{\mathrm{i,w}}\right)(K_{\mathrm{p,c}}s + K_{\mathrm{i,c}})}{\bar{V}s(s-D)(s^2 + \hat{B}K_{\mathrm{p,w}}s + \hat{B}K_{\mathrm{i,w}}) + F_4}\,, \tag{34}$$

and $L_6(s)$ is the transfer function from λ to V

$$L_6(s) = \frac{\lambda_{\mathrm{V}}(s)}{V(s)} = \frac{R\left[F_5 + F_6\left(\bar{V}s(s-D)(s^2+\hat{B}K_{\mathrm{p,w}}s+\hat{B}K_{\mathrm{i,w}})+F_4\right)\right]}{\bar{V}(s-D)\left(\bar{V}s(s-D)(s^2+\hat{B}K_{\mathrm{p,w}}s+\hat{B}K_{\mathrm{i,w}})+F_4\right)}. \tag{35}$$

with $F_5 = -R\,EB\left(K_{\mathrm{p,c}}s + K_{\mathrm{i,c}}\right)\left(F_1 s^2 + F_2 s + F_3\right)$ and $F_6 = \left(\bar{\omega}_{\mathrm{r}}/\bar{V}\right)s + \left(\bar{\omega}_{\mathrm{r}}/\bar{V}\right)D + B$.

If there is no model mismatch, $\gamma = 1$, $L_5(s)$ can be simplified and results in the same expression as $L_3(s)$

$$L_5(s)\Big|_{\gamma=1} = \frac{R\,E(K_{\mathrm{p,c}}s + K_{\mathrm{i,c}})}{\bar{V}s^2 + (R\,EK_{\mathrm{p,c}} - \bar{V}D)s + R\,EK_{\mathrm{i,c}}}. \tag{36}$$

4.5. Framework dynamics

In summary, the transfer functions $L_3(s)$ and $L_5(s)$, characterize the closed-loop dynamics of the WSE-TSR tracking control scheme and will be used in the rest of the paper to assess the ill-conditioning problem

$$L_3(s) = \frac{\hat{\lambda}_{\lambda^*}(s)}{\lambda^*(s)} = \frac{R\,E\left[s^2+\left(\hat{B}-\frac{\bar{\omega}_{\mathrm{r}}}{\bar{V}}D(1-\gamma)\right)K_{\mathrm{p,w}}s+\left(\hat{B}-\frac{\bar{\omega}_{\mathrm{r}}}{\bar{V}}D(1-\gamma)\right)K_{\mathrm{i,w}}\right](K_{\mathrm{p,c}}s+K_{\mathrm{i,c}})}{\bar{V}s(s-D)(s^2+\hat{B}K_{\mathrm{p,w}}s+\hat{B}K_{\mathrm{i,w}})+F_4}, \tag{37}$$

$$L_5(s) = \frac{\lambda_{\lambda^*}(s)}{\lambda^*(s)} = \frac{R\,E\left(s^2+\hat{B}K_{\mathrm{p,w}}s+\hat{B}K_{\mathrm{i,w}}\right)(K_{\mathrm{p,c}}s+K_{\mathrm{i,c}})}{\bar{V}s(s-D)(s^2+\hat{B}K_{\mathrm{p,w}}s+\hat{B}K_{\mathrm{i,w}})+F_4}. \tag{38}$$

5. Results

In this section, the WSE-TSR tracking control scheme is analyzed both in the time-domain and in the frequency-domain. The effect of the ill-conditioning on the scheme is studied by simulating different uncertainty levels in the modeled parameters.

5.1. Case study

In this paper, it is of interest to study a 1.5 m two-bladed H-Darrieus vertical-axis wind turbine (VAWT) [10] but the analysis can also be performed for a horizontal-axis wind turbine (HAWT). The $C_{\mathrm{p}}(\lambda)$ curve of the studied VAWT is depicted in Figure 4 for $\beta = 0°$. The optimal TSR $\lambda^* = 4$ corresponds to $C_{\mathrm{p}}^* = 0.47$.

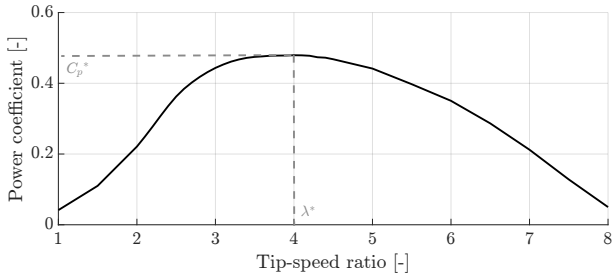

Figure 4: Power coefficient for the H-Darrieus VAWT for a pitch angle of 0° [10].

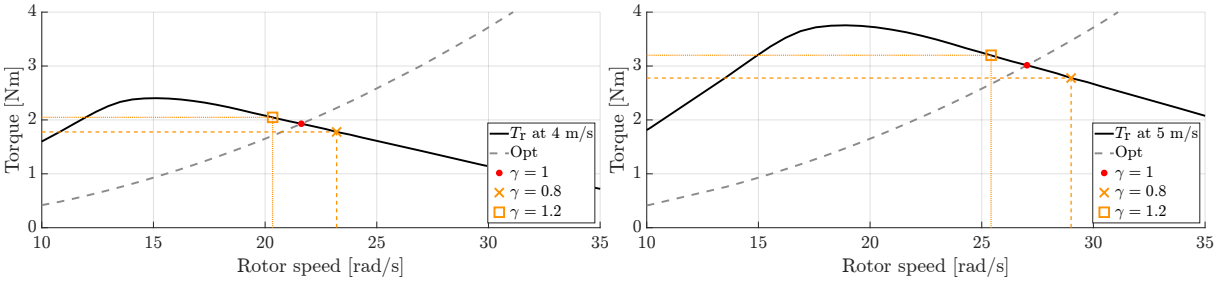

(a) Wind speed 4 m/s. (b) Wind speed 5 m/s.

Figure 5: Torque-versus-speed response of the WSE-TSR tracking control scheme.

5.2. Effect of model uncertainty

The effect of the uncertainty in the model parameters is investigated by simulating two extreme cases: $\gamma = 0.8$ and $\gamma = 1.2$. The I&I gains, $K_{\mathrm{p,w}} = 20$ and $K_{\mathrm{i,w}} = 50$, are selected and result in satisfactory estimator performance. The TSR tracker gains, $K_{\mathrm{p,c}} = -10$ and $K_{\mathrm{i,c}} = -0.5$, are tuned to achieve a balance between performance and robustness of the PI controller [4].

Figure 5 summarizes the steady-state results for two different wind speeds, *i.e.* $V = 4\,\mathrm{m/s}$ and $V = 5\,\mathrm{m/s}$. When there is no model mismatch, T_{g} matches the optimal operating condition (*i.e.* the cross-point of the aerodynamic torque and the optimal steady-state trajectory). With an uncertainty in the modeled parameters, the system moves away from the optimal condition. According to Equation (8), when the magnitude of $\hat{C}_{\mathrm{p}}$ is decreased ($\gamma = 0.8$) the wind speed is overestimated, resulting in a lower steady-state T_{g} from the TSR tracking controller. On the other hand, when $\hat{C}_{\mathrm{p}}$ used by the wind speed estimator is increased ($\gamma = 1.2$), the wind speed is underestimated and the wind turbine operates at a lower λ in reality.

Figures 6 and 7 show how these trends propagate to the other variables in the framework. In this case, the wind turbine operates under a realistic turbulent wind field with a mean wind speed of 4 m/s and a turbulence intensity of 5% for 600 s. As can be observed, $\hat{V}$ is overestimated for $\gamma = 0.8$ while it is underestimated for $\gamma = 1.2$. Thus, the controller framework tracks λ^* using the estimated feedback quantity $\hat{\lambda}$, but in reality, the turbine's actual tip-speed ratio λ has a bias to the reference value. Since the wind turbine is not operating at its optimal operating point, the aerodynamic power extraction efficiency is suboptimal. Specifically, for $\gamma = 0.8$, a reduction in power of 1 % is obtained.

These observations are further supported by inspection of the frequency response of the system closed-loop transfer functions, $L_3(s)$ and $L_5(s)$ in Figure 8. The tuning of the wind

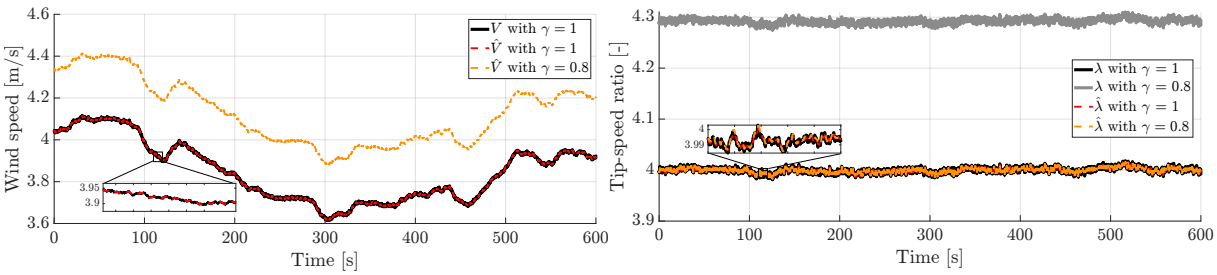

(a) Wind speed results. (b) Tip-speed ratio results.

Figure 6: Simulation results showing the wind speed and the tip-speed ratio for an underestimation of C_{p} under a realistic turbulent wind profile.

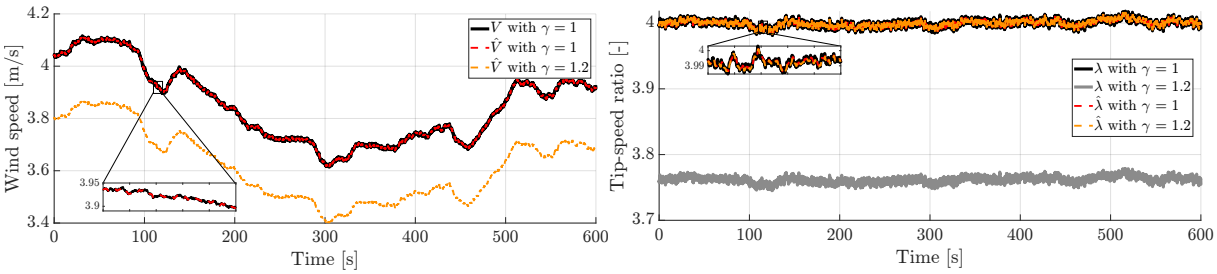

(a) Wind speed results. (b) Tip-speed ratio results.

Figure 7: Simulation results showing the wind speed and the tip-speed ratio for an overestimation of C_p under a realistic turbulent wind profile.

speed estimator gains is adapted to emphasize the effect of model uncertainty. Upon closer inspection, the frequency responses show differences in the static gains. Even with the presence of model uncertainty, the static gain of $L_3(s)$ will always be zero proving that the controller presumes to track the optimal condition (*i.e.* $\hat{\lambda} = \lambda^*$). However, in reality, the wind turbine will not operate at the point of maximum power extraction (*i.e.* $\lambda \neq \lambda^*$) as confirmed by the static gains of $L_5(s)$, which differ from zero in the presence of a model mismatch.

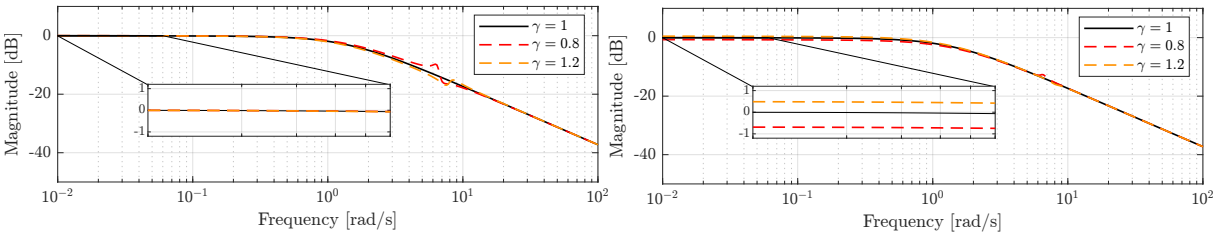

(a) $L_3(s) = \frac{\hat{\lambda}_{\lambda^*}(s)}{\lambda^*(s)}$ (b) $L_5(s) = \frac{\lambda_{\lambda^*}(s)}{\lambda^*(s)}$

Figure 8: Frequency response of the system under different model uncertainty and with an incorrect tuning of the wind speed estimator gains.

6. Conclusions

In this study, the WSE-TSR tracking controller scheme is studied in detail. Due to a lack of information in the scheme, the wind speed cannot be uniquely estimated from the product with other model parameters in the power balance equation. This results in the so-called ill-conditioning, leading to biased wind speed estimates and reduced energy capture under model uncertainty. A linear frequency-domain analysis has been performed, by deriving transfer functions characterizing the WSE-TSR tracking scheme, and are used to evaluate the problem of ill-conditioning. It is shown that uncertainty in modeled turbine parameters can lead to erroneous tracking of the optimal aerodynamic performance.

References

[1] Dalla Riva A, Hethey J ad Vitina A 2017 IEA Wind TCP Task 26 - Impacts of Wind Turbine Technology on the System Value of Wind in Europe Tech. rep.
[2] UN Climate change conference UK 2021 URL https://ukcop26.org/cop26-goals/
[3] van Kuik G A, et al. 2016 Long-term research challenges in wind energy - A research agenda by the European Academy of Wind Energy *Wind Energy Science* **1** 1-39
[4] Bossanyi E A 2000 The Design of closed loop controllers for wind turbines *Wind Energy* **3** 146-163
[5] Mulders S P, Zaaijer M V, Bos R and van Wingerden J W 2020 Wind turbine control: Open-source software for control education, standardization and compilation *J. Phys.: Conf. Series* **1452**

[6] Pao L Y and Johnson K E 2011 Control of wind turbines: approaches, challenges, and recent developments *IEEE Control Systems* **31**
[7] Bonaccorso F, Scelba G, Consoli A and Muscato G 2011 EKF - Based MPPT control for vertical axis wind turbines *IECON Proceedings (Industrial Electronics Conference)* 3614-3619
[8] Liu Y, Pamososuryo A K, Ferrari R M and van Wingerden J W 2022 The Immersion and Invariance wind speed estimator revisited and new results *IEEE Control System Letters* **6** 361-366 (*Preprint* 2104.07696)
[9] Ortega R, Mancilla-David F and Jaramillo F 2013 A globally convergent wind speed estimator for wind turbine systems *International Journal of Adaptive Control and Signal Processing* **27** 413-425
[10] LeBlanc B and Simão Ferreira C 2018 Overview and design of PitchVAWT *Wind Energy Symposium*